

# Hydroxyl-Terminated Oligomers Crosslinked by Alkoxysilane Sol-Gel or Polyurethane Chemistries: A Comparison

S. CUNEY,<sup>1</sup> J. F. GÉRARD,<sup>1</sup> M. DUMON,<sup>1</sup> J. P. PASCAULT,<sup>1</sup> G. VIGIER,<sup>2</sup> K. DUŠEK<sup>3</sup>

<sup>1</sup> Laboratoire des Matériaux Macromoléculaires UMR CNRS #5627, Institut national des Sciences Appliquées de Lyon, Bât.403, 69621 Villeurbanne, France

<sup>2</sup> GEMPPM UMR CNRS #5510, Institut national des Sciences Appliquées de Lyon, Bât.501, 69621 Villeurbanne, France

<sup>3</sup> Institute of Macromolecular Chemistry, Academy of Science of the Czech Republic, Heyrovsky Sq. 2, 162 06 Prague 6, Czech Republic

Received 19 July 1996; accepted 7 October 1996

**ABSTRACT:** The structures of *in situ* generated clusters and the level of physical interactions in two types of networks differing from the chemistry of crosslinking were studied by means of small-angle X-ray analysis and dynamic mechanical spectroscopy. For the first type of networks, the crosslinks result from the hydrolysis and condensation of ethoxysilane endgroups, thus generating silicon-rich dispersed phase. In the second case, the crosslinks result from the formation of urethane units by introducing a triol. In the two cases, different types of soft segment precursors having different polarities are considered.  $\alpha,\omega$ -hydroxyl-terminated oligomers of hydrogenated polybutadiene or polycaprolactone or a polyester from oleic acid are used. The miscibility of the soft-segment chains with the relatively polar crosslinks is the most important parameter for understanding the morphology and the mechanical behavior of such materials. The main difference obtained from the SAXS analysis and DMS experiments is that the silicon-rich clusters appear to be stiffer and well separated in comparison with the trimethylolpropane-urethane crosslinks. In addition, in the case of silica clusters generated *in situ*, the phase separation plays an important role. In the polycaprolactone-based systems, the formation of clusters is mainly governed by the nature and the reactivities of the functional groups. As a consequence, the clusters are more fractal-like. The mechanical behavior, i.e., the mechanical losses and the high-temperature behavior, is discussed as a function of the existing interactions and the concentration of elastically active network chains in the different types of networks considered.  
© 1997 John Wiley & Sons, Inc. *J Appl Polym Sci* **65**: 2373–2386, 1997

**Key words:** urethane; organic–inorganic hybrids; networks; morphology; x-ray scattering; mechanical relaxation; modulus modeling

## INTRODUCTION

In recent years, more and more attention has been paid to polymeric systems, particularly the cross-

linked ones, with *in situ* generated nanostructures. By controlled formation of these nanostructures (clusters), mechanical and other physical (electrical, optical, magnetic, etc.), properties can be tailored. We will be concerned here with so-called chemical clusters: in a chemical cluster, the constituent units are held together by covalent

Correspondence to: J.-F. Gérard, J.-P. Pascault.

*Journal of Applied Polymer Science*, Vol. 65, 2373–2386 (1997)  
© 1997 John Wiley & Sons, Inc. CCC 0021-8995/97/122373-14

bonds and represent (branched) sequences units of a certain type (e.g., "hard" units). Formation of hard segments in linear polyurethanes, which can associate into hard domains, has been known for a long time.<sup>1</sup> More recently, attention was paid to branched hard (chemical) cluster formed when a hard component having a functionality over two is considered.<sup>2,3</sup> The formation process of these clusters has been a subject of theoretical analysis<sup>4</sup> with respect to their size distribution and percolation threshold.

Formation of inorganic clusters within organic matrices (organic/inorganic hybrid systems) has been a subject of increasing interest since about a decade ago.<sup>5-9</sup> The inorganic clusters are most frequently based on siloxane structures and are generated by a sol-gel process. This one involves the hydrolysis and the condensation of alkoxy-silane groups.

The organic and inorganic hard clusters differ in several points: 1) the inorganic clusters are "harder," i.e., they do not soften in the normal temperature range; 2) the inorganic clusters are usually less "miscible" with the organic continuous phase; and 3) the inorganic (silica) clusters contain some silanol groups strongly interacting with polar groups of the organic components even if in polyurethanes the urethane groups are also active in hydrogen bonding.

These special features influence the cluster structure formation and the interactions with the continuous phase. The processing and resulting properties of the systems are controlled by the cluster structure, their volume fraction, and their arrangement in space. The main factors affecting cluster evolution are as follows<sup>2</sup>: 1) the initial composition of the system and functionality of the components<sup>2</sup>; 2) chemical reactivities of groups and reaction paths controlling the bond formation<sup>2</sup>; 3) relative diffusion rates of the clusters<sup>10,11</sup>; 4) excluded volume effects controlling the effective reactivity of functional groups; 5) tendency to association (aggregation) and phase separation of clusters; and 6) embedment of clusters in a network assigning to them a certain correlation distance.

The reactivity of the functional groups and the reaction pathways are certainly the most important factors controlling the cluster structure, because these ones are chemical entities that cannot be disintegrated physically (dissolved). However, the other physical factors can profoundly change the bond formation probabilities for the reactive groups making them dependent of the

size and shape of the clusters.<sup>12</sup> Thus, diffusion limitations usually make the distributions narrower, whereas tendencies to association resulting possibly in phase separation of liquid-liquid type enhance chemical joining of large clusters. As a result, not only the size distribution but also the internal structure of clusters changes. The control by chemical reactivity only gives loose, more or less randomly branched structures—fractal objects with fractal dimensions from 2 to 2.5, whereas phase separation yields compact nonfractal particles, possibly with a fractal surface.<sup>13,14</sup> The internal structure of clusters plays an important role in the interaction with the matrix. Loose structures can more strongly interact with the matrix than the compact ones.

Modeling of cluster formation has been a subject of several studies,<sup>15</sup> but very few studies take into account the real chemical mechanisms. In one of our previous articles,<sup>3</sup> we were dealing with a purely chemically controlled cluster evolution process in three-component polyurethanes. The same concept was later generalized to any multi-component system.<sup>4,16</sup> The exact compensation of increasing the cluster functionality and reduction of number of elastically active network chains (EANC) within the hard cluster in the framework Flory-Erman rubber elasticity theory<sup>17-19</sup> was one of the results of this analysis (cluster compensation hypothesis).<sup>3,4</sup> This compensation was predicted to be valid in a certain range of cluster evolution process, viz up to the percolation threshold of the hard structure. This prediction was in a fairly good agreement with the experimental results on polyester-urethane networks.<sup>3</sup> However, this approach is expected to fail as the cluster formation is controlled by other factors, especially by the thermodynamic aggregation (phase separation). The purpose of this article is to compare structures of clusters and the level of physical interactions, as revealed by the Small-Angle X-Ray (SAXS) analysis and from the viscoelastic properties, in two main groups of networks differing primarily in the chemistry of crosslinking then in the type of the soft segment component and the type of diisocyanate. The methods used for looking into the structure and its evolution include: 1) SAXS, giving directly the electron density fluctuation in the materials; 2) the sol fraction, characterizing the completeness or branching efficiency of the crosslinking reaction; and 3) static and dynamic mechanical properties. The static properties, such as the equilibrium modulus in the rubbery state, can be correlated

**Table I Characteristics of Macrodiols**

Abbreviation	Commercial Name	$\bar{M}_n$ (g/mol)	$I_p^a$	$T_g$ (°C) <sup>b</sup>	$\Delta C_p^b$ (J/g·K)	$T_m$ (°C) <sup>b</sup>
PCL20	CAPA 2000	2000	1.4	-72	0.53	45
HPBD	GI 2000	2100	1.5	-45	0.40	/
C36*	PRIPLAST 3197	2000	1.7	-59	0.41	/
PCL6	CAPA 200	550	1.2	-78	0.68	2
PCL10	CAPA 210	1000	1.4	-73	0.66	39
PCL20	CAPA 220	2000	1.4	-72	0.53	45
PCL30	CAPA 231		1.5	-71	0.50	53

<sup>a</sup> Determined by SEC (PS standard).

<sup>b</sup> Determined by DSC.

with the crosslink density, whereas the dynamic properties characterize the distribution of the relaxing elements, and thus, give information on the level of physical interactions in the system. In the first group of networks, the crosslinks are formed by the sol-gel reactions of ethoxysilane endgroups, whereas in the second one, the crosslinks result from the formation of urethane units from a triol. Three types of soft segment precursors of increasing polarity were considered: hydrogenated polybutadiene, a fatty acid oligoester, and polycaprolactone. Moreover, the precursor chains before crosslinking differed in the number of urethane groups, by which the physical interactions have been altered. In addition, the validity of cluster compensation hypothesis on equilibrium modulus has been tested for such systems. It should be remarked that in all inorganic/organic hybrid systems considered, the content of the inorganic component did not exceed 2%; thus, reinforcement effect due to the presence of the inorganic filler is negligible.

## EXPERIMENTAL

### Materials

$\alpha,\omega$ -Hydroxyl-terminated oligomers (soft segments, denoted SS) used are as follows (Table I): (a) polycaprolactone (PCL) of molar mass from 550 to 3000 g·mol<sup>-1</sup> (CAPA<sup>®</sup>, from Solvay Co.); (b) hydrogenated polybutadiene (HPBD) of molar mass of 2000 g·mol<sup>-1</sup> (from Nippon-Soda Co.); (c) a polyester diol (C36\* or PRIPLAST 3197<sup>®</sup>, from Unichema Intern. Co.) of molar mass 2000 g·mol<sup>-1</sup>, resulting from the reaction of one molecule of an oleic acid dimer (PRIPOL 1009) with two molecules of the corresponding diol (PRIPOL 2033).

The following diisocyanates (DI) have been used (Table II): (a) 1,3-bis-2,2'-(2-isocyanatopropyl)benzene (mTMXDI, from Amer. Cyanamid Co.), and (b) dicyclohexylmethane diisocyanate (H<sub>12</sub>MDI, from Bayer Co.).

2-Ethyl-2-hydroxyethyl-1,3-propanediol or trimethylolpropane (TMP) was used as a crosslinking agent for PU networks; ( $\gamma$ -aminopropyl)triethoxysilane ( $\gamma$ -APS), ( $\gamma$ -amino propyl)methyldiethoxysilane ( $\gamma$ -APMDES), and ( $\gamma$ -isocyanatopropyl)triethoxysilane ( $\gamma$ -IPS) were used for functionalization of SS endgroups designed for sol-gel crosslinking chemistry (Table II).

### Sample Designation and Processing

The code indicates the component abbreviation and the molar ratios of groups. For example, PCL1000-TMXDI-TMP 1,3,4/3 refers a PU network based on: (a) 1 mol of polycaprolactone having a molar mass of 1000 g·mol<sup>-1</sup>, 3 mol of TMXDI, and 4/3 mol of TMP.

Table III gives the formulations considered in this article. Networks having the same SS content have been compared: this is why the NCO-to-OH ratios are different for the networks crosslinked by alkoxy silane and urethane-based chemistries.

The synthesis of PU and hybrid networks is schematically given in Figure 1. In the first step of the synthesis of the hybrid organic-inorganic materials, an alkoxy silane-endcapped oligomer has been prepared: (a) for the endcapped macrodiols, 2 mol of  $\gamma$ -IPS were reacted with one mole of macrodiol at 80°C for 24 h under a nitrogen atmosphere; (b) for endcapped oligo-urethanes, SS/H<sub>12</sub>MDI/ethoxysilane, first, 1 mol of macrodiol was reacted at 80°C with 2 mol of diisocyanate. After complete reaction, the prepolymer was dissolved in THF and the  $\gamma$ -aminosilane ( $\gamma$ -APS or

**Table II** Characteristics of Chain Extenders, Crosslinking Agents, Organo-Silanes, and Diisocyanates

Abbreviation	Commercial Name	M (g/mol)	$T_g$ (°C)
TMP	$\begin{array}{c} \text{CH}_2\text{OH} \\   \\ \text{CH}_3-\text{CH}_2-\text{C}-\text{CH}_2-\text{OH} \\   \\ \text{CH}_2\text{OH} \end{array}$	134	-54
NPG	$\begin{array}{c} \text{CH}_3 \\   \\ \text{HO}-\text{CH}_2-\text{C}-\text{CH}_2-\text{OH} \\   \\ \text{CH}_3 \end{array}$	104	/
$\gamma$ -APS	$\begin{array}{c} \text{OC}_2\text{H}_5 \\   \\ \text{NH}_2-(\text{CH}_2)_3-\text{Si}-\text{OC}_2\text{H}_5 \\   \\ \text{OC}_2\text{H}_5 \end{array}$	221	/
$\gamma$ -APMDES	$\begin{array}{c} \text{OC}_2\text{H}_5 \\   \\ \text{NH}_2-(\text{CH}_2)_3-\text{Si}-\text{OC}_2\text{H}_5 \\   \\ \text{CH}_3 \end{array}$	191	/
$\text{H}_{12}$ MDI	$\text{O}=\text{C}=\text{N}-\text{C}_6\text{H}_{10}-\text{CH}_2-\text{C}_6\text{H}_{10}-\text{N}=\text{C}=\text{O}$	262	-73
<i>m</i> -TMXDI	$\begin{array}{c} \text{CH}_3 \quad \quad \quad \text{CH}_3 \\   \quad \quad \quad   \\ \text{O}=\text{C}=\text{N}-\text{C}-\text{C}_6\text{H}_4-\text{C}-\text{N}=\text{C}=\text{O} \\   \quad \quad \quad   \\ \text{CH}_3 \quad \quad \quad \text{CH}_3 \end{array}$	244	-89
$\gamma$ -IPS	$\begin{array}{c} \text{OC}_2\text{H}_5 \\   \\ \text{O}=\text{C}=\text{N}-(\text{CH}_2)_3-\text{Si}-\text{OC}_2\text{H}_5 \\   \\ \text{OC}_2\text{H}_5 \end{array}$	248	/

$\gamma$ -APMDES) was added dropwise at room temperature. After 1 h of reaction, the solvent was removed under reduced pressure.

The final network was obtained in the absence of a solvent by hydrolysis and condensation of the ethoxysilane groups by the addition of a trifluoroacetic acid (TFA) solution. The conditions are as follows: 0.1 mol % TFA for SS/ $\text{H}_{12}$ MDI/ $\gamma$ -APS oligomers; 0.5 mol % TFA for PCL20/ $\gamma$ -IPS oligomer; 5 mol % TFA for HPBD/ $\gamma$ -IPS and C36\*/ $\gamma$ -IPS oligomers.

After stirring at room temperature, the mixture was cast into a mold and cured for 24 h at 100°C under pressure. The SS/ $\text{H}_{12}$ MDI/ $\gamma$ -APS networks were then postcured at 150°C for 12 h.

The polyurethane networks were obtained in two stages. One mol of macrodiol was reacted with 3 mol of diisocyanate at 80°C. After the reaction was completed, 0.01 wt % of dibutyltin dilaurate (catalyst) was added followed by TMP. After stirring at room temperature, the mixture was cast into a mold and cured at 100°C under pressure. All the PU networks were postcured at 120°C for 12 h.

#### Sample Characterization

The sol content in the networks was determined by extraction at room temperature in tetrahydrofuran (THF). The weight ratio of THF to

**Table III Synthesized Hybrid and Polyurethane Networks**

Formulation	Soft Segment Content (% wt.)
PCL20- $\gamma$ -IPS 1-2	79
C36*- $\gamma$ -IPS 1-2	75
HPBD- $\gamma$ -IPS 1-2	82
PCL20-H <sub>12</sub> MDI- $\gamma$ -APS 1-2-2	67
C36*-H <sub>12</sub> MDI- $\gamma$ -APS 1-2-2	62
HPBD-H <sub>12</sub> MDI- $\gamma$ -APS 1-2-2	71
PCL20-H <sub>12</sub> MDI- $\gamma$ -APMDES 1-2-2	69
C36*-H <sub>12</sub> MDI- $\gamma$ -APMDES 1-2-2	63
HPBD-H <sub>12</sub> MDI- $\gamma$ -APMDES 1-2-2	73
PCL30- <i>m</i> TMXDI-TMP 1-3-4/3	84
PCL20- <i>m</i> TMXDI-TMP 1-3-4/3	69
PCL10- <i>m</i> TMXDI-TMP 1-3-4/3	63
PCL6- <i>m</i> TMXDI-TMP 1-3-4/3	38
HPBD- <i>m</i> -TMXDI-TMP 1-3-4/3	73
PCL30-H <sub>12</sub> MDI-TMP 1-3-4/3	83
PCL20-H <sub>12</sub> MDI-TMP 1-3-4/3	67
PCL10-H <sub>12</sub> MDI-TMP 1-3-4/3	62
PCL6-H <sub>12</sub> MDI-TMP 1-3-4/3	36
HPBD-H <sub>12</sub> MDI-TMP 1-3-4/3	71
C36*-H <sub>12</sub> MDI-TMP 1-3-4/3	62

the polymer was 100 : 1. After 1 week, the extracted polymer was dried and its mass was determined. The sol fraction,  $w_s$ , was calculated using the relation:

$$w_s = 100(1 - m_d/m_0)$$

where  $m_d$  is the mass of the dry residue and  $m_0$  is initial mass of the polymer.

Differential Scanning Calorimetry (DSC) thermograms were recorded using a Mettler TA3000 instrument, with a heating rate of 7.5 K·min<sup>-1</sup> in argon. The glass transition temperature at the onset,  $T_g$ , and the change in calorific capacity,  $\Delta C_p$ , at the glass transition were also measured.

Dynamic mechanical properties were measured by the means of the dynamic analyzer RSAII (Rheometrics) operating in the tension mode. A frequency of 10 Hz was used to study the temperature dependence of the dynamic mechanical properties in the range from -50 to 200°C. The equilibrium moduli in the relaxation mode were also measured for a deformation of 2%. The temperature has been chosen in order that the sample will be in the rubbery state, i.e., out of the  $\alpha$ -relaxation region (80° above  $T_g$ ).

Small angle X-ray scattering (SAXS) experi-

ments were performed with a setup including a rotating anode X-ray generator with copper target and nickel filter ( $\lambda = 1.54 \text{ \AA}$ ), a point collimation produced mainly by two orthogonal mirrors, and a line position sensitive proportional counter connected to a computer. The scattered intensity,  $I$ , in the angular range  $0.02 < 2q < 0.05$  ( $2q$  being the scattering angle in radian) was obtained as a function of the scattering vector  $q$ :  $q = (4\pi/\lambda) \sin \Theta$ . The correlation length,  $d_c$ , is directly calculated from the position of the maximum and the Porod radius,  $R_p$ , is calculated as the ratio of integrated intensity to the Porod' constant assuming an asymptotic behavior ( $q^{-4}$ ). Using Beaucage' formalism,<sup>20</sup> the Guinier radius, a theoretical correlation length,  $\xi$ , and a correlation intensity factor,  $k$  ( $0 < k < 6$ ), were computed. The latter parameter,  $k$ , is a measure of the degree of particle order in the material. The higher  $k$  is, the more ordered the particle dispersion is.

## RESULTS AND DISCUSSION

### Morphologies by SAXS Measurements

As briefly discussed in the Introduction, the structures generated in the system from the physical interactions and the chemical reactions can have either a characteristic size and can be more or less regularly distributed in the SS matrix, or the structures are looser and have a wide distribution of self-similar shapes. The former systems exhibit distinct maxima on the SAXS scattering curve. The scattering intensity further depends on the difference in electron density (Table IV); thus, the silica clusters formed by the sol-gel reaction are "seen" better than the organic clusters. The most characteristic feature of these systems was a curve with maximum scattering and, therefore, the SAXS data were evaluated according to the two-phase model further assuming that the inclusions have a spherical shape.

The scattering curves are displayed in Figure 2, and the characteristic parameters of the model are summarized in Table V. Where the application of the two-phase model is questionable and the structures appear to be loose, the corresponding data are enclosed between parenthesis. Among the materials variables listed above, it is clearly seen that the polarity (miscibility) of the SS has the major influence. The HPBD-based networks always exhibit a two-phase behavior and the correlation intensity factor  $k$  is high. Simi-

Figure 1. Network synthesis

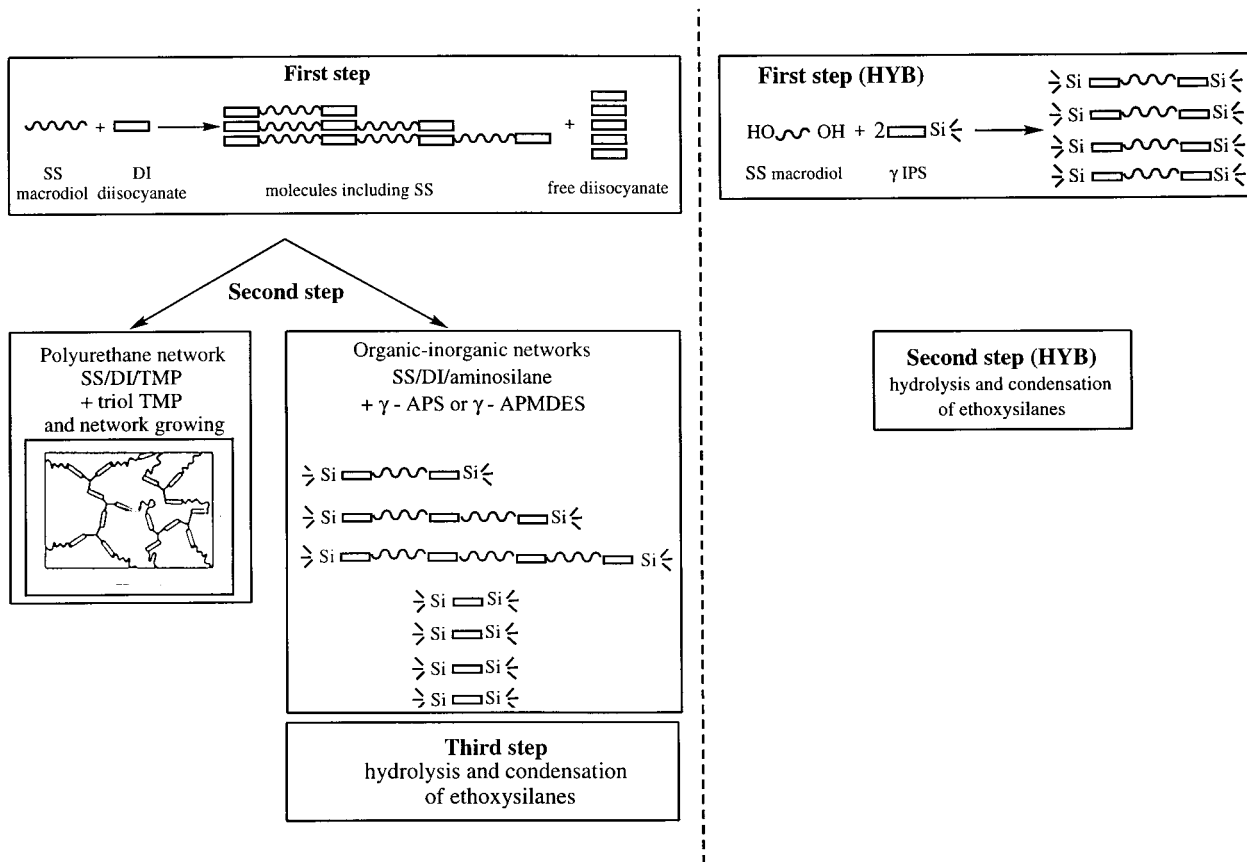


Figure 1 Pathways for synthesizing the two types of networks.

larly, the scattering behavior of the fatty acid polyester C36\*-systems corresponds more to a two-phase system, whereas the scattering from the C36\*/H<sub>12</sub>MDI/ $\gamma$ -APS system seems to be more diffuse and looks like the PCL-based material ones. The polycaprolactone samples exhibit the presence of relatively diffuse structures or even do not exhibit any scattering. Thus, there is no basic difference in the morphology between the networks obtained from the hydrolysis and the condensation of HPBD/ $\gamma$ -IPS or HPBD/DI/ $\gamma$ -APS and the HPBD-based polyurethane cross-linked by TMP.

Differences, however, exist in the particle radii and the correlation distances. The endgroups of the SS/ $\gamma$ -IPS networks form smaller particles (0.7–0.8 nm in radius). The correlation distance corresponds roughly to the end-to-end distance of the precursor chains in agreement with the results found by Rodrigues et al.<sup>14</sup> The clusters in HPBD hybrid polyurethanes or in TMP-cross-linked HPBD polyurethanes are about two times

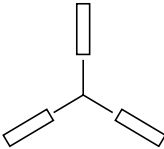
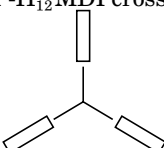
larger ( $R_p = 1.5$ – $2.5$  nm) and their correlation distance is about 7–10 nm. This feature is an indication that some endgroups form physical clusters before crosslinking and that this cluster formation is assisted by the presence of diisocyanate endcapped molecules. Some other endgroups must be isolated in space and dispersed irregularly.

The SS/H<sub>12</sub>MDI/ $\gamma$ -APS-based networks exhibit an asymptotic scattering behavior with a  $q^{-4}$  law, which justifies the calculation of Porod radii. The SS/H<sub>12</sub>MDI/ $\gamma$ -APMDES networks also display the same asymptotic behavior except the PCL-based network because of a very weak scattering due to an almost homogeneous structure. The asymptotic behavior PCL20/ $\gamma$ -IPS networks cannot be fitted by a  $q^{-4}$  law, which means either a smooth interface, a fractal dimension, or both.

### Sol Fractions

Because the reactions have been carried out to high conversions, the sol fractions are expected to

**Table IV Electronic Density and Solubility Parameters of the Different Components in PU Networks**

Components	Electronic Density <sup>a</sup> (mol · électrons. cm <sup>-3</sup> )	Solubility Parameter <sup>b</sup> (MPa <sup>1/2</sup> )
HPBD	0.5	17
C36*	0.53	19
PCL20	0.57	21
TMP- <i>m</i> TMXDI crosslink 	0.62	23
TMP-H <sub>12</sub> MDI crosslink 	0.61	25

<sup>a</sup> Calculated with Müller's method.

<sup>b</sup> Average values calculated with Fedors tables: hydroxy end groups in macrodiols are not taken into account.

be low (about 1% or less). It is the case in most polyurethanes, except of HPBD/*m*-TMXDI/TMP 1-3-4/3 (8%).

The hybrid systems based on PCL soft segments also satisfy more or less this limit (2%), but for the HPBD and C36\*-systems the sol fractions are higher (6 to 9%). Originally, the reactive ethoxysilane chain ends are apolar and mix reasonably well with polybutadiene or the fatty acid polyester. As soon as hydrolysis starts, these chain ends have the tendency to associate. In the associated regions, the hydrolysis (and condensation) rate even increases. However, a part of chain ends remains unhydrolyzed (apolar) for some time and interdispersed in the HPBD matrix. They possibly hydrolyze later when they cannot associate due to the formed covalent network. The condensation is mostly intermolecular. In general, a high degree of condensation is characteristic for hydrolysis and condensation of alkoxy-silanes: a conversion of about 80% of ethoxysilane groups has been found in tetraethoxysilane (TEOS) gels mainly due to small ring formation.<sup>16</sup> Thus, SS molecules with partly hydrolyzed and cyclized endgroups represent extractable material. This interpretation is supported by the fact that the sol is composed of single precursor molecules and some corresponding to dimers. A much wider dis-

tribution of molecular masses, which would correspond to the determined sol fractions, is absent.

## Viscoelastic Properties

### Mechanical Losses

Dynamic mechanical measurements allow us to characterize the local mobilities and their changes due to physical interactions and, in the limit of low frequencies/high temperatures, to get a value close to the equilibrium modulus determined by the concentration of elastically active network chains (EANC). Well phase-separated systems usually behave more simply than systems with loose and interpenetrating hard clusters. Our phase-separated systems should exhibit one relaxation region characterized by a single mechanical loss peak that may be somewhat widened or a shoulder may appear due to the existence of interphase regions. The relaxation of the separated phase is not seen in the considered temperature range. The existence of loose one-phase interpenetrating structure should result in wider, asymmetric, or bimodal relaxation regions.

The most important results are summarized in Figures 3 and 4. Again, the most important parameter is the nature (polarity) of the SS compo-

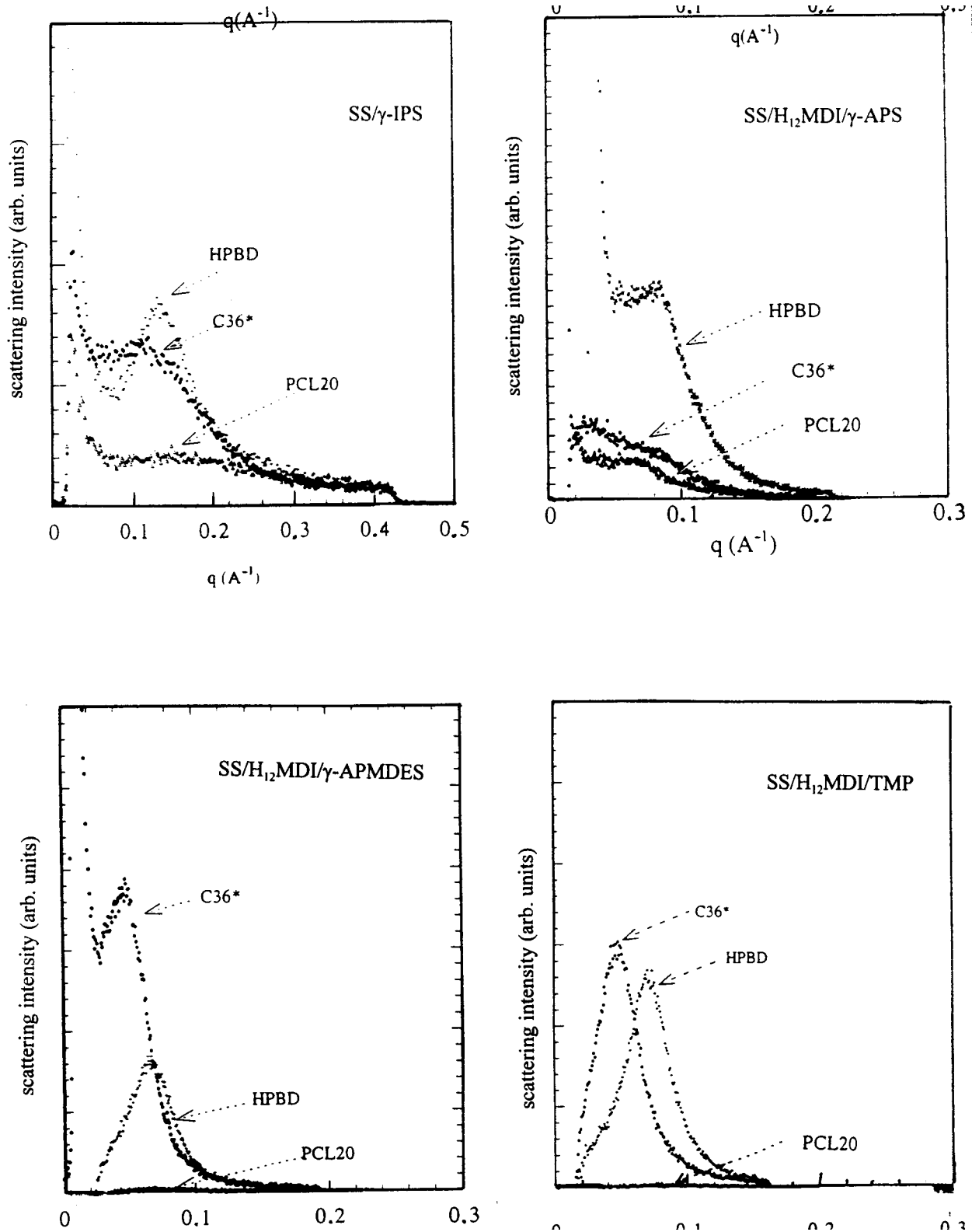


Figure 2 SAXS profiles for the various types of systems.



**Table V Parameters Characterizing the Morphology Obtained from SAXS**

Formulation	Particle Size		Correlation Length		Correlation Intensity $k$
	$R_p$ (Å)	$R_g$ (Å)	$d_c$ (Å)	$\zeta$ (Å)	
HPBD- $\gamma$ -IPS	7	9	48	39	3.1
C36*- $\gamma$ -IPS	8	10	56	34	1
PCL20- $\gamma$ -IPS	/	5	42	30	0.7)
HPBD/H <sub>12</sub> MDI/ $\gamma$ -APS	16	21	100	82	1.8
C36*/H <sub>12</sub> MDI/ $\gamma$ -APS	(15	27	81	/	/)
PCL20/H <sub>12</sub> MDI/ $\gamma$ -APS	(17	22	84	70	1.5)
HPBD/H <sub>12</sub> MDI/ $\gamma$ -APMDES	16	24	92	74	4.4
C36*/H <sub>12</sub> MDI/ $\gamma$ -APMDES	24	32	126	94	2.5
PCL20/H <sub>12</sub> MDI/ $\gamma$ -APMDES			No scattering		
HPBD-H <sub>12</sub> MDI-TMP	15	21	88	74	5.4
C36*-H <sub>12</sub> MDI-TMP	22	28	132	104	3.1
HPBD- <i>m</i> -TMXDI-TMP	13	21	77	61	4.4
PCL20- <i>m</i> TMXDI-TMP			No scattering		
PCL20-H <sub>12</sub> MDI-TMP			No scattering		
PCL6- <i>m</i> TMXDI-TMP			No scattering		
PCL6-H <sub>12</sub> MDI-TMP			No scattering		

$R_p$ : Porod's radius as obtained from the scattering curves.

$R_g$ : Guinier's radius as obtained from Beaucage's formalism.

$d_c$ : correlation length as obtained from Bragg's law.

$\zeta$ : theoretical correlation length as obtained from Beaucage's formalism.

$k$ : correlation intensity factor.

ment. Hydrogenated polybutadiene-based systems exhibit the sharpest loss peaks and a little change in their position on temperature scale. On the other hand, the PCL systems are characterized by the copolymer effect and cluster–matrix interactions, resulting in large shifts of the  $\tan \delta$  maxima, peak widening, and possibly even bimodality. The behavior of C36\*-systems is specific, pointing sometimes to the existence of phase-separated domains, sometimes to strong interactions between soft and hard structures.

The SS/ $\gamma$ -IPS systems exhibit one loss peak that becomes wider and more asymmetric towards higher temperature in the series of SS: HPBD-C36\*-PCL20, i.e., with increasing polarity of SS and, therefore, stronger interactions with the silanol–siloxane clusters.

The ethoxysilane-encapped polyurethanes exhibit somewhat a more complex behavior than the simpler SS/ $\gamma$ -IPS-based systems. The widening of the loss tangent peak towards higher temperatures is much more extensive and a second maximum can occur on the loss curve. Presumably, this is due to interactions of the urethane groups and clusters with the silanol–siloxane clusters or with themselves.

The TMP-crosslinked polyurethanes with PCL

and partly C36\* soft segments exhibit strong interactions characterized by wide but simple loss peaks and a shift of their maximum due to a copolymer effect. This is closer to a classical behavior observed with “ideal” polyurethane networks peaks. It is also interesting to examine differences caused by the type of the diisocyanate used. No large difference can be noticed in the case of HPBD systems. In strongly interacting PCL/DI/TMP systems, the loss peak is much wider in the case of H<sub>12</sub>MDI-based materials, with a maximum shifted to higher temperatures by about 20 K. This effect is due to the fact that the hard clusters are more intimately penetrated by the soft matrix.

### High-Temperature Moduli

The high-temperature storage moduli should be close to equilibrium moduli,  $E_{eq}$ , which can be correlated with the concentrations of elastically active network chains (EANC). It is always true, given that the frequency of 10 Hz is still high. For such a frequency, strongly interacting and slowly relaxing entities of units can contribute to the storage modulus,  $E'$ , up to the temperature region for which degradation starts. If  $E'$  is determined only by covalent crosslinks and measured sufficiently far

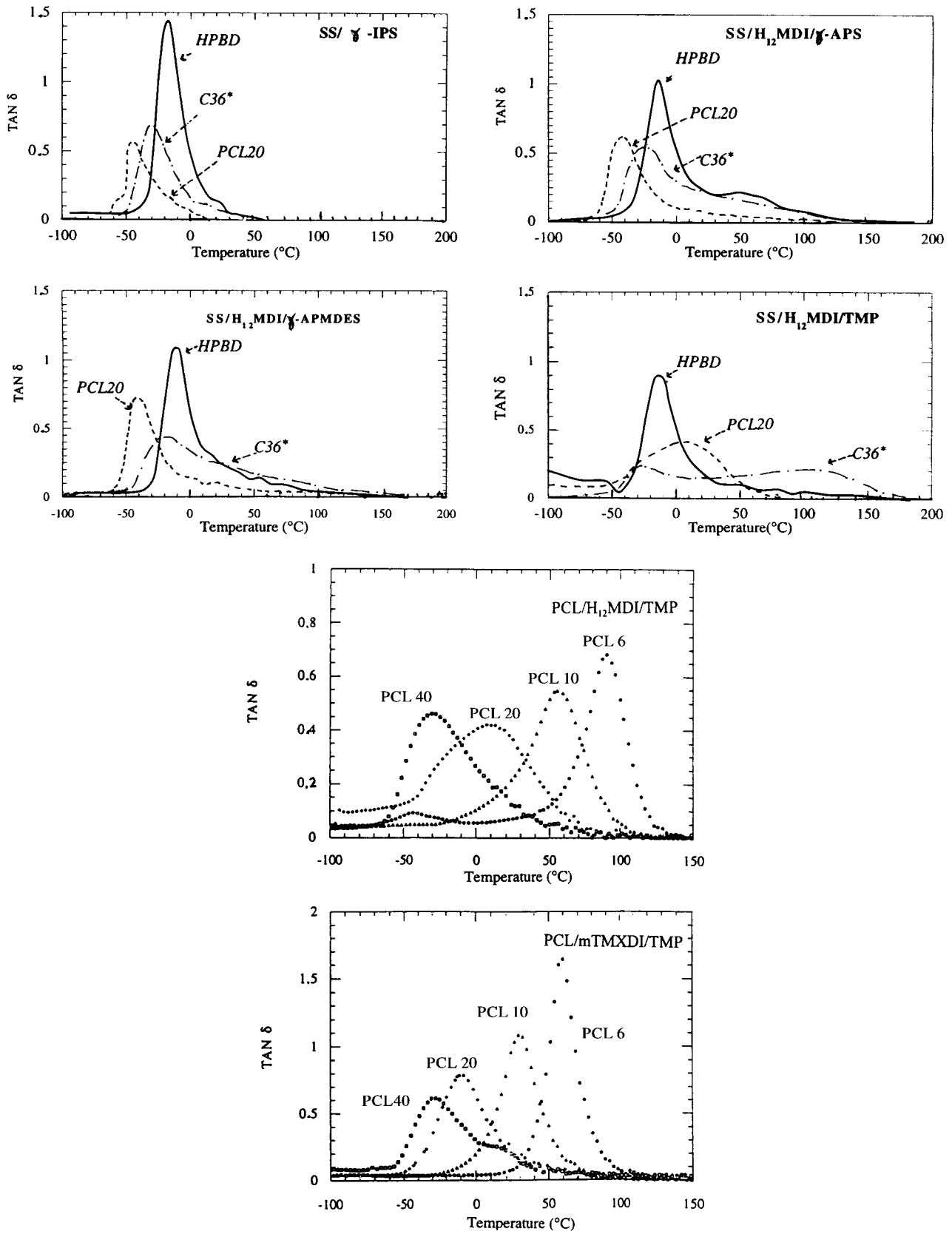


**Figure 3** Dependence of the loss factor,  $\tan \delta$ , with the temperature for the various crosslinked systems at 10 Hz.

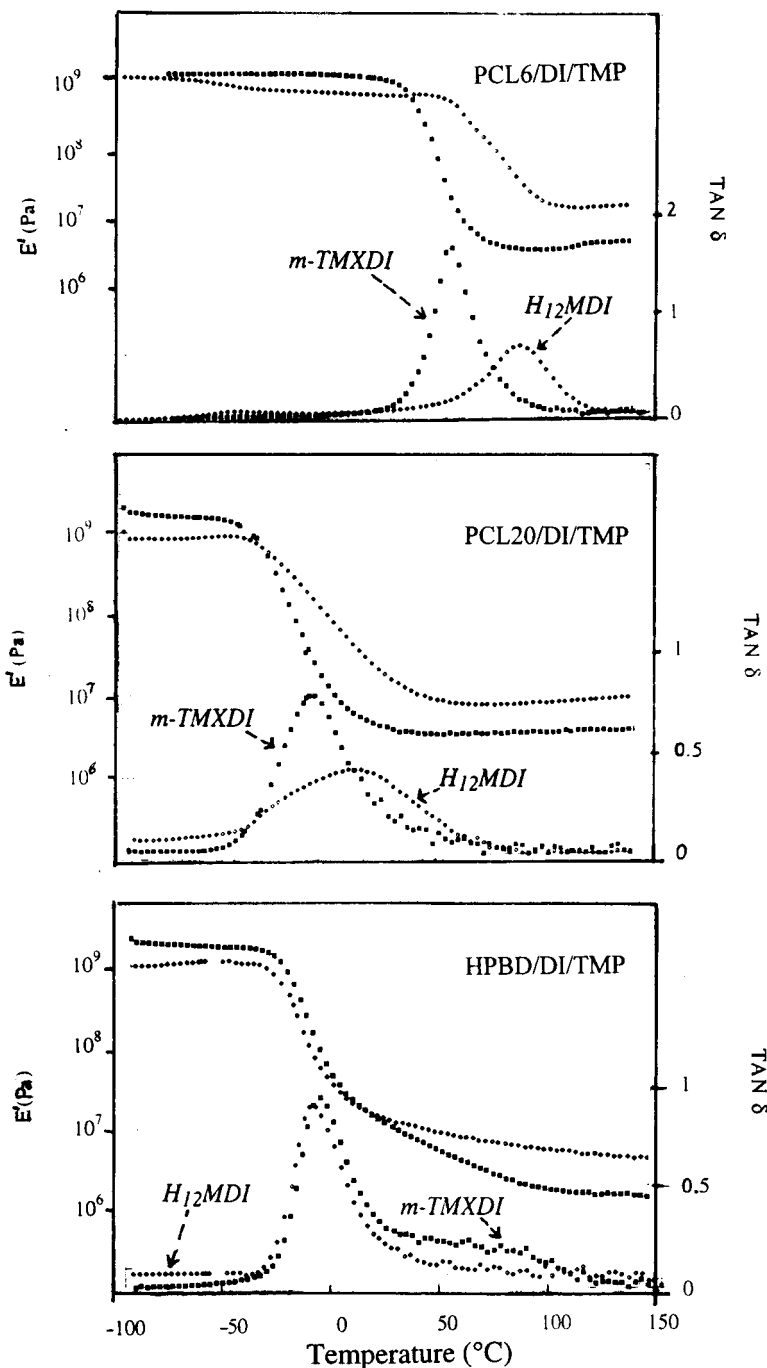


**Figure 4** Dynamic mechanical spectra (i.e., storage modulus and  $\tan \delta$  vs. temperature) of various systems at 10 Hz.

from the glass transition region, it increases with increasing temperature, because the modulus is proportional to absolute temperature,  $T$ . This criterion disqualifies for some of the systems, because  $E'$  rather decreases with increasing  $T$ . Among them are most of HPBD and also C36\*-based systems (HPBD/ $H_{12}$ MDI/TMP, HPBD/ $m$ -TMXDI/

TMP, HPBD/ $H_{12}$ MDI/ $\gamma$ -APMDES, C36\*/ $H_{12}$ MDI/TMP, and C36\*/ $H_{12}$ MDI/ $\gamma$ -APMDES) (see Fig. 4 as an example—HPBD/DI/TMP systems). The values of the relaxed moduli are summarized in Table VI.

The moduli of samples that did show up an increase rather than a decrease of  $E'$  in the rub-

**Table VI Selected Relaxed and Theoretical Equilibrium Moduli for the SS/ $\gamma$ -IPS and SS/DI/aminosilane Systems**

System	$E'$ Relaxed (MPa)	Calculated $E$ (MPa)
HPBD/ $\gamma$ -IPS	3.8	4.4
C36*/ $\gamma$ -IPS	3.4	4.6
PCL20/ $\gamma$ -IPS	3.8	4.4
PCL20/H <sub>12</sub> MDI/ $\gamma$ -APS	6.5	2.6
PCL20/ $\gamma$ -APMDES	4.0	2.6
PCL30/H <sub>12</sub> MDI/TMP	4.7	1.5
PCL20/H <sub>12</sub> MDI/TMP	5.9	2.4
PCL10/H <sub>12</sub> MDI/TMP	7.9	3.9
PCL6/H <sub>12</sub> MDI/TMP	9.1	5.4
PCL30/ <i>m</i> -TMXDI/TMP	2.4	1.8
PCL20/ <i>m</i> -TMXDI/TMP	2.6	2.7
PCL10/ <i>m</i> -TMXDI/TMP	3.1	4.1
PCL6/ <i>m</i> -TMXDI/TMP	3.3	5.2

bery region were analyzed with respect to the theoretical value expected by considering the system as being crosslinked by hard clusters.<sup>2-4,14</sup> In the multicomponent networks composed of units that can be considered soft and hard, hard chemical clusters are formed in which hard units are linked together. The DI/TMP networks as well as the hybrids crosslinked from the sol-gel chemistry can belong to this category. If the cluster buildup is determined solely by the chemical reactivity of functional groups and physical aggregation/phase separation phenomena are absent, the cluster size distribution can be described by simple (statistical or kinetic) branching theories.<sup>4</sup> The implication of cluster existence for equilibrium rubber elasticity is the following: the connections between active branch points within the hard clusters are too short with respect to the soft chains, so that their extensions resulting from external deformation can be neglected. Thus, the chains between active branch points within hard clusters should not be counted, at least for small strains. On the other hand, there exist a cluster functionality distribution ranging from the value for the chemical crosslink (here equal to 3) up to infinity. There has been found an interesting and generally valid implication of the cluster existence within the framework of the Flory–Erman junction–fluctuation theory.<sup>17-19</sup> Below the percolation (gelation) threshold of the hard clusters, the decrease in the number of EANC (by locking some of them within the cluster) is fully compensated by increasing functionality of the cluster crosslink. This is because below this threshold, the cy-

cle rank of the hard structure is zero. This theorem was tested quite successfully on a number of polyurethane networks.<sup>3</sup> However, it should be stressed that within the framework of the F-E theory the cluster crosslinks are still considered as small (pointlike) multifunctional junctions. The compensation theorem is invalid in the case where the clusters grow big close to or beyond their percolation threshold. Beyond that point, the continuous hard structure is becoming to dominate the mechanical behavior more and more.

The systems discussed here are all be beyond the percolation threshold if the crosslinking is ideal. The term ideal means here that the reactivities of all groups are equal, no cycles are formed, and branching is not restricted by any physical interactions. Moreover, in our case, it is assumed that functional groups react to full completion. Some of these assumptions are evidently not fulfilled. Making a reasonable assumption that the cluster functionality is high enough, the theoretical value of the equilibrium modulus can be calculated from the concentration of soft chains. Under this condition, the moduli calculated for the phantom network as well as the affine network are equal (Table VI). For  $\gamma$ -IPS networks the agreement is relatively good. As follows from the morphology studies discussed above, the cluster crosslinks are relatively small and the hard structure is evidently well below the percolation threshold. The experimental values are lower for the reasons discussed above in connection with the sol fraction: existence of single or double chain-end clusters not contributing to the equilibrium elasticity.

Quite different results are obtained for polyurethane systems crosslinked with TMP or through alkoxy silane chain ends. The experimental moduli are often higher than those that would correspond only to the SS chains. This is due to the fact that their morphological structure is quite different: larger clusters, poorer correlations in space, percolation-type clusters rather than the compact ones. Two main reasons for this discrepancy can be put forward: 1) some interactions involving urethane and silanol groups are so strong that they do not relax fully under the given conditions and, 2) the systems are beyond the percolation threshold of the hard structure. The latter argument is applicable for the "homogeneous" PCL systems where the cluster size distribution is

expected to be controlled mainly by the chemical branching process. Some of the clusters are evidently quite large and their deformation contributes to the retractive force, so that the SS chains do not act independently any longer, some of them possibly being locked in the hard structures. This picture can also explain the differences between the H<sub>12</sub>MDI and mTMXDI systems. The H<sub>12</sub>MDI-based urethane structures seem to interact somewhat more strongly with the SS chains than in the case of mTMXDI, as wider loss peaks are displayed in Figure 4. Therefore, in H<sub>12</sub>MDI systems, the deformation of the hard structure may play an important role. This is well evidenced by the difference in ultimate properties:

	strain at break, %	stress at break, MPa
PCL10/TMXDI/TMP	800	17
PCL10/H <sub>12</sub> MDI/TMP	200	15

The higher degree of connectivity of the hard structure in H<sub>12</sub>MDI systems makes them more brittle.

## CONCLUSIONS

In all systems discussed above, the existence of hard clusters of different shapes and compactness controls their mechanical behavior. The miscibility of the soft-segment chains with the relatively polar crosslink or chain extender units appears to be the most important factor. The hydrogenated polybutadiene chains are less compatible than the polycaprolactones. From the point of view of the crosslink clusters, the silica ones are quite stiff and well separated, whereas the trimethylolpropane-urethane crosslinks are relatively well interpenetrated by polycaprolactone chains. From the SAXS analysis, it follows that in the case of the formation of silica crosslinks by the sol-gel chemistry, the phase-separation control plays an important role on the final morphology. The generated clusters are compact and more regularly dispersed. In polycaprolactone-based polyurethanes, the cluster formation is much more determined by composition and the reactivities of the functional groups and the clusters are more fractal-like. This phenomenon indicates that the percolation threshold for the hard structure has been approached or surpassed.

The dynamic mechanical properties indicate relatively weak silica cluster-matrix interactions, increasing, however, by passing from the nonpolar HPBD to more polar PCL. In systems with polyurethane groups and their combination with silica-silanol formations, the interactions can be quite strong and complicated extending over several tens of Kelvins.

One could ask a simple question: for the same soft component, is the sol-gel or the polyurethane crosslinking chemistry better? The answer is not easy, according to the fact that it depends on the nature of the SS. For the HPBD systems, it seems that the introduction of urethane groups into the sol-gel crosslinking system does not bring any improvement. Because of the low silica content of all our materials, PU-networks seem to be better candidates than hybrid networks in terms of mechanical properties. An improvement of the hybrid networks can be obtained by using a higher silica content.

## REFERENCES

1. S. L. Cooper and R. W. Seymour, *Macromolecules*, **6**, 49 (1973).
2. K. Dušek, in *Telechelic Polymers*, E. J. Goethals, Ed., CRC Press, Boca Raton, FL, 1988, p. 289.
3. B. Nabeth, J. P. Pascault, and K. Dušek, *J. Polym. Sci., Polym. Phys.*, **34**, 1031 (1996).

4. K. Dušek and J. Somvarsky, *Faraday Disc.*, **101**, to appear.
5. J. E. Mark, C. Y. Lee, and P. A. Bianconi, *Hybrid Organic-Inorganic Composites*, Advances in Chemistry series 585, American Chemical Society, Washington, DC, 1995; and references therein.
6. C. Sanchez and F. Ribot, *N. J. Chem.*, 1007 (1994).
7. A. Serier, J. P. Pascault, and T. M. Lam, *J. Polym. Sci. Chem.*, **29**, 1125 (1991).
8. H. Kaddami, F. Surivet, J. F. Gerard, T. M. Lam, and J. P. Pascault, *J. Inorg. Organomet. Polym.*, **4**, 183 (1994).
9. S. Cuney, J. F. Gerard, J.-P. Pascault, and G. Vigier, in *Better Ceramics Through Chemistry VII—Organic/Inorganic Hybrid Materials*, Edts B. K. Coltrain, D. W. Schaefer, C. Sanchez, and G. K. Wilkes, MRS Publ., **435**, 143 (1996).
10. T. A. Vilgis and G. Heinrich, *Macromol. Theory Simul.*, **3**, 271 (1994).
11. K. Kang and S. Redner, *Phys. Rev.*, **A32**, 435 (1985).
12. M. R. Landry, B. K. Coltrain, C. J. T. Landry, and J. M. O'Reilly, *J. Polym. Sci., Polym. Phys. Ed.*, **33**, 637 (1995).
13. C. J. Brinker and G. W. Scherer, in *Sol-Gel Science: The Physics and Chemistry of Sol-Gel Processing*, Academic Press, London, 1990, p. 908.
14. D. E. Rodrigues, A. B. Brennan, C. Betrabet, B. Wang, and G. L. Wilkes, *Chem. Mater.*, **4**, 1437 (1992).
15. F. Family and D. P. Landau, Eds., *Kinetics of Aggregation and Gelation*, North Holland, Amsterdam, 1984.
16. K. Dušek and J. Somvarsky, *Macromol. Chem. Phys., Macromol. Symp.*, **106**, 119 (1996).
17. B. Erman and P. J. Flory, *J. Chem. Phys.*, **68**, 5363 (1978).
18. P. J. Flory and B. Erman, *Macromolecules*, **15**, 800 (1982).
19. J. P. Questel and J. E. Mark, in *Comprehensive Polymer Science*, Vol 2, Pergamon Press, New York, 1989, p. 271.
20. G. Beaucage and D. W. Schaefer, *J. Noncryst. Solids*, **173**, 797 (1994).